ISSN 1674-1056
http://cpb.iphy.ac.cn
http://iopscience.iop.org/cpb
中国物理 B
Chinese Physics
中国物理
Chinese Physics B

Effect of transient space-charge perturbation on carrier transport in high-resistance CdZnTe semiconductor

Yu Guo(郭玉), Gang-Qiang Zha(查钢强), Ying-Rui Li(李颖锐), Ting-Ting Tan(谭婷婷), Hao Zhu(朱昊), Sen Wu(吴森)
Citation: Chin. Phys. B . 2019, 28(11): 117201 . **doi:** 10.1088/1674-1056/ab43bb
Journal homepage: http://cpb.iphy.ac.cn; http://iopscience.iop.org/cpb

What follows is a list of articles you may be interested in

Temporal pulsed x-ray response of CdZnTe:In detector

Rong-Rong Guo(郭榕榕), Ya-Dong Xu(徐亚东), Gang-Qiang Zha(查钢强), Tao Wang(王涛), Wan-Qi Jie(介万奇)
Chin. Phys. B . 2018, 27(12): 127202 . **doi:** 10.1088/1674-1056/27/12/127202

Twin boundary dominated electric field distribution in CdZnTe detectors

Jiangpeng Dong(董江鹏), Wanqi Jie(介万奇), Jingyi Yu(余竞一), Rongrong Guo(郭榕榕), Christian Teichert, Kevin-P Gradwohl, Bin-Bin Zhang(张滨滨), Xiangxiang Luo(罗翔祥), Shouzhi Xi(席守智), Yadong Xu(徐亚东)
Chin. Phys. B . 2018, 27(11): 117202 . **doi:** 10.1088/1674-1056/27/11/117202

Modeling capacitance–voltage characteristic of TiW/p-InP Schottky barrier diode

Yi-Dong Wang(王一栋), Jun Chen(陈俊)
Chin. Phys. B . 2018, 27(9): 097203 . **doi:** 10.1088/1674-1056/27/9/097203

Multi-carrier transport in $ZrTe_5$ film

Fangdong Tang(汤方栋), Peipei Wang(王培培), Peng Wang(王鹏), Yuan Gan(甘远), Le Wang(王乐), Wei Zhang(张威), Liyuan Zhang(张立源)
Chin. Phys. B . 2018, 27(8): 087307 . **doi:** 10.1088/1674-1056/27/8/087307

Structural and electrical properties of laser-crystallized nanocrystalline Ge films and nanocrystalline Ge/SiN_x multilayers

Li Cong, Xu Jun, Li Wei, Jiang Xiao-Fan, Sun Sheng-Hua, Xu Ling, Chen Kun-Ji
Chin. Phys. B . 2013, 22(10): 107201 . **doi:** 10.1088/1674-1056/22/10/107201

Effect of transient space-charge perturbation on carrier transport in high-resistance CdZnTe semiconductor*

Yu Guo(郭玉), Gang-Qiang Zha(查钢强)†, Ying-Rui Li(李颖锐), Ting-Ting Tan(谭婷婷), Hao Zhu(朱昊), and Sen Wu(吴森)

MIIT Key Laboratory of Radiation Detection Materials and Devices, State Key Laboratory of Solidification Processing, School of Materials Science and Engineering, Northwestern Polytechnical University (NWPU), *Xi'an* 710072, *China*

(Received 24 June 2019; revised manuscript received 5 September 2019; published online 16 October 2019)

The polarization effect introduced by electric field deformation is the most important bottleneck of CdZnTe detector in x-ray imaging. Currently, most of studies focus on electric field deformation caused by trapped carriers; the perturbation of electric field due to drifting carriers has been rarely reported. In this study, the effect of transient space-charge perturbation on carrier transport in a CdZnTe semiconductor is evaluated by using the laser-beam-induced current (LBIC) technique. Cusps appear in the current curves of CdZnTe detectors with different carrier transport performances under intense excitation, indicating the deformation of electric field. The current signals under different excitations are compared. The results suggest that with the increase of excitation, the amplitude of cusp increases and the electron transient time gradually decreases. The distortion in electric field is independent of carrier transport performance of detector. Transient space-charge perturbation is responsible for the pulse shape and affects the carrier transport process.

Keywords: CdZnTe, transient space-charge perturbation, laser-beam-induced current (LBIC) technique, carrier transport

PACS: 72.80.Ey, 73.50.Gr, 73.61.Ga, 72.20.Jv **DOI:** 10.1088/1674-1056/ab43bb

1. Introduction

High-resistivity semiconductor CdZnTe is the most promising material for room-temperature nuclear radiation detector because of its high atomic number, large bandgap, and excellent carrier transport characteristics.[1–4] It is widely used in astrophysics, medical imaging, security imaging, industrial testing, and other fields.[5–7] However, polarization at high x-ray fluxes has become the focus of relevant studies in recent years, restricting the development of CdZnTe detector in some fields such as medical imaging requiring high photon flux.[8] Bale revealed that CdZnTe detector with a low hole mobility suffered a buildup of positive space charge as a result of trapped holes, which collapsed the internal electric field.[9] James *et al.* studied bias-induced polarizations of CdZnTe detectors with different contacts by using transient-current technique combined with the relationship between defect level depth and Fermi level.[10] Franc *et al.* evaluated the effect of 1200-nm pulsed mode infrared light on the polarization of CdZnTe detector.[11] The results showed that the use of 1200-nm LED achieved the depolarization by promoting the detrapping of holes. Franc *et al.* reported the effect of sub-band light on CdZnTe detectors under the irradiation of 943-nm LED that imitates x-rays.[12] Energy levels of 0.5 eV, 0.7 eV, and 0.8 eV are responsible for the polarization of CdZnTe detectors. These studies focused on the deformation of electric field caused by trapped carriers. However, the perturbation of electric field in CdZnTe detector due to drifting carriers has been rarely reported. Transient space charge of drifting photon-generated carriers themselves results in the deformation of electric field as studied in solid materials such as iodine.[13,14] To better understand the polarization of CdZnTe radiation detector, in this paper the space-charge perturbation in CdZnTe detector is studied.

Time-of-flight technique (TOF) has been widely used to obtain the information about carrier transport properties and distribution of electric field inside a crystal.[14–16] Alpha source, x-ray machine, and γ-ray source, which are commonly used in the TOF measurements, usually have the disadvantage of random uncertainty. Therefore, in this study, a pulsed laser is used as an excitation source; this laser has good monochromaticity and can be easily controlled to systematically study the effect of space-charge perturbation on carrier transport process in CdZnTe semiconductor. It is found that the current signals of different detectors all have a cusp under an intense optical excitation. The current signals under different power illuminations are measured to study the effect of space-charge perturbation on carrier transport. Finally, the space-charge perturbation effect is analyzed, and the number of photogen-

*Project supported by the National Natural Science Foundation of China (Grant No. 61874089), the Fund of MIIT (Grant No. MJ-2017-F-05), the 111 Project of China (Grant No. B08040), the NPU Foundation for Fundamental Research, China, and the Research Found of the State Key Laboratory of Solidification Processing (NWPU), China.

†Corresponding author. E-mail: zha_gq@nwpu.edu.cn

© 2019 Chinese Physical Society and IOP Publishing Ltd

erated carriers and pulse energy are also calculated.

2. Experiment

The n-type CdZnTe samples were cut from different parts of the same crystal ingot, and each sample has dimensions of 16.6 mm×4.4 mm×1.5 mm. The crystals were grown using the modified vertical Bridgman method. The samples were first roughly polished using an MgO suspension and then finely polished with a solution of silica sol and hydrogen peroxide. To eliminate the surface mechanical damage, a 2% bromine in methanol solution was used for chemically polishing the samples. Then, Au electrodes were deposited on both faces of samples by vacuum evaporation, and the electrode thickness was small enough (60 nm–80 nm) to avoid large reflection and absorption loss during incident light penetration on the front end material into the crystal. Then, passivation treatment was performed by using a 30% H_2O_2 solution to minimize the surface leakage of current. Finally, the samples were bonded to the substrate by using a conductive paste to form a planar CdZnTe detector.

The charge transport properties of CdZnTe detectors were evaluated by γ-ray spectra through using uncollimated ^{241}Am@59.5-keV γ-ray as the radiation source. The measurements were carried out by placing the samples inside a shielding box. The γ-ray spectra were collected by applying different voltages.

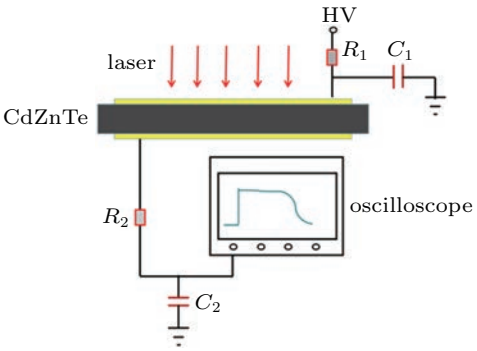


Fig. 1. Setup of laser-beam-induced current measurement.

Figure 1 shows a block diagram of the setup used for measuring the laser-beam-induced current (LBIC). The penetration depth of laser with a wavelength of 527 nm used in the experiment is much smaller than the crystal thickness. In that case, the current signals of electrons were obtained with cathode irradiation. The laser pulse width is 8 ps, much smaller than the drifting time of carriers in the crystal. In addition, the laser has the energy of 1 mJ/ pulse and a frequency of 1 Hz. Neutral density filters were used to adjust the luminous efficacy of laser, on the assumption that the initial flux of laser is I_0. To avoid the interference of current signals generated by the side of crystal, an aperture stop with a size of Φ100 μm was performed to reduce spot. The transient current signals were recorded by using an oscilloscope with a bandwidth of 1 GHz. Resistor R_1 is used to protect the circuit, and capacitor C_1 is used to filter out the ripple noise from the voltage source. Resistors R_2 and C_2 are added as an equivalent input circuit of the oscilloscope. All the LBIC measurements were operated at 20 °C.

3. Results and discussion

Figure 2 shows the LBIC waveforms of different CdZnTe detectors at a power illumination of $I = I_0 \times 10^{-3}$ for different bias voltages, ranging from 200 V to 400 V. Figure 3 shows the $(\mu\tau)_e$ of detectors CZT1 and CZT2 obtained by fitting the γ-ray energy spectra under different bias voltages using the Hetch equation. A clear cusp appears in the waveforms of two detectors with different charge transport performances.

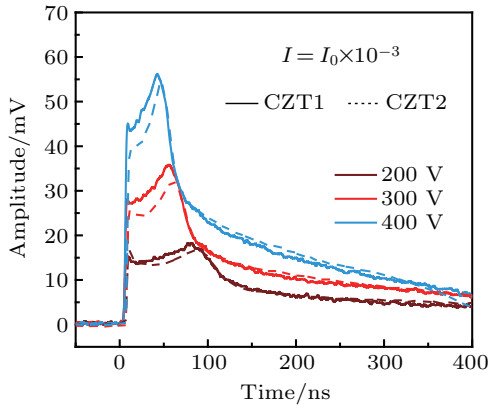


Fig. 2. LBIC results of detectors CZT1 and CZT2 illuminated by $I = I_0 \times 10^{-3}$ from cathode side.

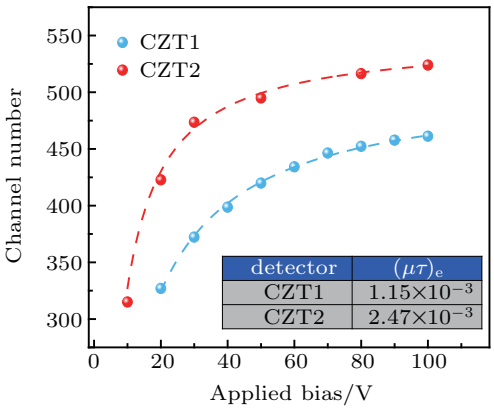


Fig. 3. Fitting results of $(\mu\tau)_e$ for detectors CZT1 and CZT2.

The generation of the cusp is due to the fact that the electric field in crystal is distorted. The deformation of electric field can be attributed to two reasons. The first reason may be the polarization due to poor electron transport performance. Electrons are trapped by defects in the crystal during transport, thus forming a negative space charge region that perturbs the internal electric field of crystal. The second reason of the deformation of electric field is due to the transient space-charge

perturbation. Quite a large number of generated carriers under a large light power form a transient single carrier drifting area that disturbs the electric field as well. Figure 3 shows that the cusp of current waveform does not affect the electric field distortion caused by poor electron transport characteristics.

To further verify the second reason, the LBIC waveforms of one selected CdZnTe detector were measured under different illumination powers, ranging from $I = I_0 \times 10^{-5}$ to $I = I_0 \times 10^{-3}$, and the results are shown in Fig. 4.

Under a low illumination power ($I = I_0 \times 10^{-5}$), the drift of electrons across the sample (uniform field distribution) produces a constant current. However, a cusp can be observed under the illumination of $I = I_0 \times 10^{-4}$. As the illumination power increases, the amplitude of cusp increases and electron transient time decreases. Therefore, the cusp in the curve can be attributed to the transient space-charge perturbation effect.[17–19] Under a higher excitation, more carriers are generated whose self-field is large enough to perturb the internal electric field of detectors.

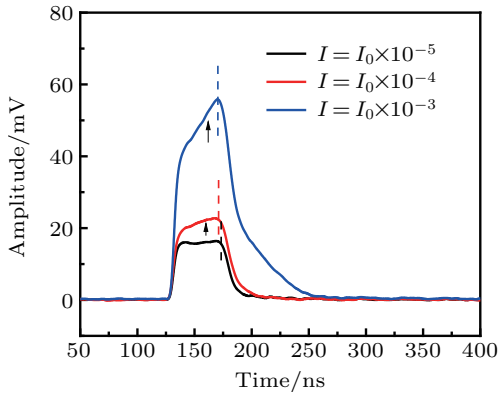


Fig. 4. Curves of LBIC waveform amplitude *versus* time with different illumination powers from cathode side under 400-V bias voltage.

Figure 5 shows a schematic diagram of transient space-charge effect perturbation, where λ is the penetration depth, L is the crystal thickness, v is the drift velocity of electron, and V is the applied bias voltage. With cathode irradiation, a narrow electron drifting region was formed after the generated carriers have been recombined between $X = 0$ and $X = \lambda$. The drifting region acts as the space-charge region when a very large number of carriers are generated.

On the assumption that there are N electrons in the transient space-charge region, the region moving to $X = x'$ perturbs the electric field. Hence, the electric field strengths $\boldsymbol{E_1}$ and $\boldsymbol{E_2}$ as indicated in Fig. 5 can be expressed as[18]

$$E_1(d') = E_0 - \frac{4\pi Nq}{\varepsilon A}\left(1 - \frac{x'}{L}\right), \tag{1}$$

$$E_2(d') = E_0 + \frac{4\pi Nq}{\varepsilon A}\frac{x'}{L}, \tag{2}$$

where N is the number of electrons in the carrier drifting region, q is the unit charge, A is the surface area, $\boldsymbol{E}$ is the applied electric field strength, and ε is the dielectric constant of CdZnTe crystal.

The internal electric field strength within the crystal is related to the number of carriers N in the transient space-charge region. When the incident light power is small, the transient space-charge perturbation effect can be ignored. However, when the light power is so large that the self-field of space charge region is close to the applied electric field strength E, the electric field around the transient charge region $\boldsymbol{E}_1$ is not equal to $\boldsymbol{E}_2$. Therefore, under intense optical excitation, the electrons in the front of the electron cloud are present in the strong electric field $\boldsymbol{E}_2$ and accelerate the drifting, thus rapidly increasing the current signal. When most of the faster electrons drift away, the current curve shows a significant drop.

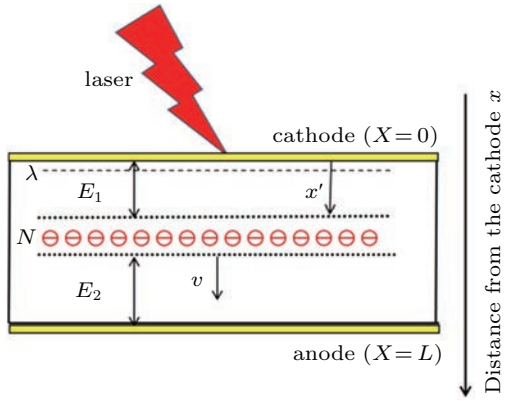


Fig. 5. Principle of transient space-charge effect.

A typical cusp appears at $\sim 0.8t_r$ (t_r is the electron transient time), when the self-electric field strength is half the applied electric field strength,[20,21] where the transient space-charge effect is not negligible. In this case, the number of carriers N generated in the CdZnTe detector is calculated to be 4.42×10^8 when the applied bias voltage was 400 V.

Under a small illumination power as shown in Fig. 4, the capacitance and resistance are consistent with the oscilloscope impedance in the LBIC measurement circuit. Therefore, the charge quantity carried by a capacitor can be expressed as

$$V = nq/C, \tag{3}$$

where V is the voltage signal of oscilloscope, C is the capacitance of capacitor, n is the number of charges carried by the capacitor, and q is the quantity of unit charge.

At a bias voltage of 400 V, the voltage signal of oscilloscope is 16 mV as shown in Fig. 4, and the capacitance of capacitor C_2 is 10 pF. Using Eq. (3), n is calculated to be 1.0×10^6. As shown in Fig. 1, the number of charges carried by the capacitor is equal to the number of generated carries collected by the anode electrode of CdZnTe detector. Therefore, the number of carriers generated in the detector is

1.0×10^6 on the assumption that carrier trapping and detrapping are neglected, far less than the above calculated N. Therefore, no cusp is observed in Fig. 4. According to the proportional relationship of light intensity, the number of carriers at $I = I_0 \times 10^{-3}$ and $I = I_0 \times 10^{-4}$ are close to the calculated N. Therefore, the transient space-charge perturbation effect is not negligible in these cases and further affects the charge transport process.

When testing and analyzing the semiconductor materials, α particle and γ source are the common radiation sources for measuring the detector performance besides laser. When the CdZnTe detector is irradiated by a ray with the energy of E, the ray energy is quickly absorbed by the crystal, and a large number of electron–hole pairs are generated inside the crystal. The number of electron–hole pairs is equal to the ray energy E divided by the average energy E_{pair} required to generate a pair of electron–hole pairs, 4.64 eV for CdZnTe crystal.[22] When the transient space-charge perturbation effect is not negligible as mentioned above, the ray energy E is estimated at 3.28×10^{-10} J, and the irradiation power is calculated to be 4.1×10^4 J/s. This slightly affects the detector energy spectrum test where 5.48-MeV ^{241}Am α source and 59.5-keV γ ray are generally applied. However, it influences the x-ray fast response and the TOF measurements to a certain degree. For a 60-keV x-ray source, 4.64 eV is required to generate a pair of electron–hole pairs, so 3.4×10^{11} cps counting rate is required when 4×10^8 carriers are generated in 100 ns, where the transient space-charge is not negligible in the sample. For this case, the counting rate should be 5×10^9 cps/mm^2 on the assumption that the space charge is within 0.1-mm depth. The effect of drifting carriers should be considered to obtain the actual current information.

In previous studies of polarization of CdZnTe detectors at high x-ray fluxes, the acquisition time of Pockels effect, which is widely used, is much larger than the carrier transient time without consideration of space-charge perturbation effect. However, the above experiments indicate that the drifting carriers affect the carrier transport process and further affect the electric field of crystals, thus resulting in the polarization of CdZnTe detector. To obtain the actual information about carrier performance, a low excitation intensity should be adopted.

4. Conclusions

By using laser-beam-induced current technique, the effect of transient space-charge perturbation on the charge transport of CdZnTe detectors is investigated. Cusps can be observed in the LBIC waveforms at a larger excitation of two detectors with different values of $(\mu\tau)_e$, further indicating that the deformation of electric field is not caused by poor carrier transport performance. The current pulse signals under different laser illumination powers show that as the excitation intensity increases, the amplitude of cusp becomes larger, which, combined with the decrease in transient time, further verifies that the transient space-charge perturbation is responsible for signal shape. With intense optical excitation, a narrow drifting region composed of a large number of electrons disturbs the internal electric field of detectors and further affects the carrier transport process. When the transient space-charge is not negligible in the sample, the counting rate is 3.4×10^{11} cps for a 60-keV x-ray source.

References

[1] Schlesinger T E, Toney J E, Yoon H, Lee E Y, Brunett B A, Franks L and James R B 2001 *Mater. Sci. Eng. R* **32** 103

[2] James R B, Brunett B, Heffelfinger J, Van Scyoc J, Lund J, Doty F P, Lingren C L, Olsen R, Cross E, Hermon H, Yoon H, Hilton N, Schieber M, Lee E Y, Toney J, Schlesinger T E, Goorsky M, Yao W, Chen H and Burgeret A 1998 *J. Electron. Mater.* **27** 788

[3] Guo R R, Jie W Q, Zha G Q, Xu Y D, Feng T, Wang Tao and Du Z T 2015 *Chin. Phys. B* **24** 067203

[4] Zha G Q, Wang T and Xu Y D 2013 *Physics* **42** 862 (in Chinese)

[5] Sellin P J 2003 *Nucl. Instrum. Methods Phys. Res. A* **513** 332

[6] Cui Y, Wright G W, Ma X, Chattopadhyay K, James R B and Burgera A 2001 *J. Electron. Mater.* **30** 774

[7] Scheiber C and Giacos G C 2001 *Nucl. Instrum. Methods Phys. Res. A* **458** 12

[8] Szeles C, Soldner S A, Vydrin S, Graves J and Bale D S 2008 *IEEE Trans. Nucl. Sci.* **55** 572

[9] Bale D S and Szeles C 2008 *J. Phys. Rev. B* **77** 035205

[10] Uxa Š, Belas E, Grill R, Praus P and James R B 2013 *J. Phys. D: Appl. Phys.* **46** 395102

[11] Dědič V, Franc J, Rejhon M, Grill R, Zázvorka J and Sellin P J 2015 *Appl. Phys. Lett.* **107** 032105

[12] Franc J, Dědič V, Zázvorka J, Hakl M, Grill R and Sellin P J 2013 *J. Phys. D: Appl. Phys.* **46** 235306

[13] Suzuki K, Ichinohe Y and Seto S 2018 *J. Electron. Mater.* **47** 4332

[14] Erichson J C, Yao H W, James R B, Erickson J C, Yao H W, James R B, Hermon H and Greaves M 2000 *J. Electron. Mater.* **29** 699

[15] Dong J P, Jie W Q, Yu J Y, Guo R R, Teichert C, Gradwohl K P, Zhang B B, Luo X X, Xi S Z and Xu Y D 2018 *Chin. Phys. B* **27** 117202

[16] Guo R R, Xu Y D, Zha G Q, Wang T and Jie W Q 2018 *Chin. Phys. B* **27** 127202

[17] Li H Y, Duan L, Li C, Wang L D and Qiu Y 2014 *J. Org. Electron.* **15** 524

[18] Spear W E 1969 *J. Non-Cryst. Solids* **1** 197

[19] Many A and Rakavy G 1962 *J. Phys. Rev.* **126** 1980

[20] Papadakis A C 1967 *J. Phys. Chem. Solids* **28** 641

[21] Gibbons D J and Papadakis A C 1968 *J. Phys. Chem. Solids* **29** 115

[22] Ishii M and Kobayashi M 1992 *Prog. Cryst. Growth Charact. Mater.* **23** 245